A Linear FEM Benchmark for the Homogenization of the Eddy Currents in Laminated Media in 3D

K. Hollaus * **M. Huber** * **J. Schöberl** * **P. Hamberger** **

* *Institute for Analysis and Scientific Computing, Vienna University of Technology, 1040 Wien, Wiedner Hauptstraße 8-10, Austria (e-mail: karl.hollaus@tuwien.ac.at)*
** *Siemens Transformers Austria GmbH & Co KG, Austria (e-mail: peter.hamberger@siemens.com)*

Abstract: The simulation of eddy current losses in laminated iron cores by the finite element method is of great interest in designing of electrical machines. Modeling each lamination individually by the finite element method requires many elements and leads to an inappropriately large system of equations. A two-scale finite element method is proposed to efficiently compute the losses in laminated media with linear material properties. The approach for the two-scale finite element method based on the magnetic vector potential $\boldsymbol{A}$ is described. Its accuracy and the computational costs are evaluated by a representative linear finite element benchmark.

Keywords: Benchmark examples, eddy current analysis, electromagnetic devices, finite elements, homogenization, laminated media, multi-scale finite element method, numerical analysis.

1. INTRODUCTION

An efficient and accurate simulation of the eddy current losses in laminated cores is still a challenging task (Nogawa et al. (2006); Silva et al. (1995); Hollaus and Bíró (1999)). Modeling each laminate individually is not a feasible. Many elements have to be used in such a model leading to large systems of equations.

Homogenization overcomes the problem. Brute force methods apply either an anisotropic electric conductivity (Silva et al. (1995); Kaimori et al. (2007); Hollaus and Bíró (1999)) or prescribe a current vector potential having a single component normal to the lamination (Jack and Mecrow (1987)) in finite element models. These methods consider the eddy currents caused by the magnetic stray flux, which is normal to the lamination. The associated eddy current losses are to small because the losses caused by the main magnetic flux parallel to the lamination are neglected. Therefore, this solution is frequently corrected in a second step exploiting different approaches. Examples are Hollaus and Bíró (1999) for a 1D and Hollaus and Bíró (2000) and Bíró et al. (2005) for a 3D correction, respectively.

Strictly speaking, the total magnetic field can not be decomposed into a magnetic stray flux and into a main magnetic flux. Consequently the methods mentioned above fail. Homogenization methods, where the main magnetic flux is considered directly, have been proposed employing a magnetic scalar potential (De Rochebrune et al. (1990)) or a magnetic vector potential (Shin and Lee (1997)), respectively. Both methods are able to solve static magnetic fields. Homogenization methods for eddy current problems have been developed in Dular et al. (2003) and Krähenbühl et al. (2004), respectively. The method described in Dular et al. (2003) enforces a symmetric magnetic flux density distribution across the laminates. This restriction has been eliminated in Krähenbühl et al. (2004).

The homogenization method presented in this work is based on multi-scale finite element method (FEM) and determines a continuous tangential magnetic field intensity $\boldsymbol{H}_t$ across the interface between the laminated media and air. Contrary to Dular et al. (2003) and Krähenbühl et al. (2004) it accounts for an air gap between the conducting sheets. In the present work an approach for a two-scale finite element method (TSFEM) has been developed for the magnetic vector potential $\boldsymbol{A}$ describing the eddy currents in laminated conducting materials with linear material properties. The method is capable to treat a laminated media efficiently as a bulk without the necessity to model the laminations individually. The method requires only a matrix-vector and a vector-vector multiplication to calculate the losses. Only linear material properties are considered. The accuracy and the computational costs of the TSFEM have been studied by a reference solution of a linear FEM benchmark problem.

2. EDDY CURRENT PROBLEM

The eddy current problem to be solved in this work is described in the following, see Figure 1. It consists of a laminated material Ω_m enclosed by air Ω_0, i.e., $\Omega = \Omega_m \cup \Omega_0$ (see Fig. 1). The material parameters λ_0, λ_1 and λ_2 as shown in Fig. 1 are valid in air, in the laminations and in the gap between them, respectively, and stand for the magnetic permeability μ and conductivity σ, respectively. There are n laminations in Ω_m, each of them may exhibit several material parameters. The thickness of

a laminate is denoted by d_1 and the width of the gap by d_2. The laminated medium is assumed to be constructed periodically. A fill factor f is defined as

$$f = \frac{d_1}{d_1 + d_2}, \tag{1}$$

wherein

$$d = d_1 + d_2 \tag{2}$$

is the length of the period.

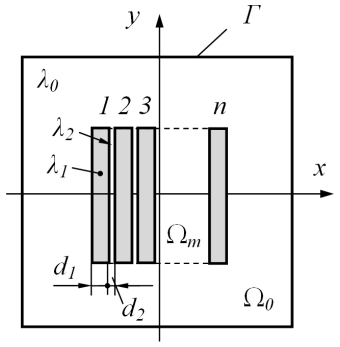

Fig. 1. Draft of the boundary value problem with a laminated medium, top view

The electric conductivity σ and the magnetic permeability μ are assumed to be linear. On the boundary $\Gamma = \Gamma_H \cup \Gamma_B$ either the tangential component of the magnetic field intensity $\boldsymbol{H}_t$ on Γ_H or the normal component of the magnetic flux density $\boldsymbol{B}_n$ on Γ_B is prescribed. The time harmonic case in the steady state is considered. Due to these assumptions Maxwell's equations have been considered in the complex representation, where j stands for the imaginary unit and ω for the angular frequency:

$$\begin{aligned}
\operatorname{curl} \boldsymbol{H} &= \boldsymbol{J} \quad \text{in } \Omega_m && (3)\\
\operatorname{curl} \boldsymbol{E} &= -j\omega \boldsymbol{B} && (4)\\
\operatorname{div} \boldsymbol{B} &= 0 && (5)\\
\boldsymbol{J} &= \sigma \boldsymbol{E} && (6)\\
\boldsymbol{B} &= \mu \boldsymbol{H} && (7)\\
\operatorname{curl} \boldsymbol{H} &= \boldsymbol{J}_0 \quad \text{in } \Omega_0 && (8)\\
\operatorname{div} \boldsymbol{B} &= 0 && (9)\\
\boldsymbol{B} &= \mu \boldsymbol{H} && (10)\\
\boldsymbol{H} \times \boldsymbol{n} &= \boldsymbol{K} \quad \text{on } \Gamma_H && (11)\\
\boldsymbol{B} \cdot \boldsymbol{n} &= b \quad \text{on } \Gamma_B && (12)
\end{aligned}$$

Relations (3) to (7) are valid in Ω_m, whereas (8) to (10) belong to air Ω_0 and (11, 12) are boundary conditions, where $\boldsymbol{K}$ is the surface current density and b means the normal component of the magnetic flux density on the surface, both are given. Due to (5) and (9) the magnetic vector potential $\boldsymbol{A}$ can be introduced as

$$\boldsymbol{B} = \operatorname{curl} \boldsymbol{A}.$$

With the aid of Faraday's law (4), the electric field intensity $\boldsymbol{E}$ is written as

$$\boldsymbol{E} = -j\omega \boldsymbol{A}.$$

Inserting this into Ampere's law (3) leads to the partial differential equation

$$\operatorname{curl} \mu^{-1} \operatorname{curl} \mathbf{A} + j\omega\sigma \mathbf{A} = \boldsymbol{J}_0 \text{ in } \Omega \tag{13}$$

with the impressed current density $\boldsymbol{J}_0$. Introducing $\boldsymbol{A}$ in (11) and (12) yields the boundary conditions

$$\mu^{-1} \operatorname{curl} \boldsymbol{A} \times \boldsymbol{n} = \boldsymbol{K} \text{ on } \Gamma_H \tag{14}$$

$$\boldsymbol{A} \times \boldsymbol{n} = \boldsymbol{\alpha} \text{ on } \Gamma_B, \tag{15}$$

where $\boldsymbol{\alpha}$ describes the normal component of the magnetic flux density. For the *Linear FEM Benchmark* described in section 4 only homogeneous boundary conditions have been applied.

2.1 Weak form

Multiplying (13) by test functions $\boldsymbol{v}$ and integrating over Ω yields

$$\int_\Omega \operatorname{curl} \mu^{-1} \ \operatorname{curl} \boldsymbol{A}\boldsymbol{v} \ d\Omega + j\omega \int_\Omega \sigma \boldsymbol{A}\boldsymbol{v} \ d\Omega = \int_{\Omega_0} \boldsymbol{J}_0 \boldsymbol{v} \ d\Omega. \tag{16}$$

Integration by parts leads to the weak form of the eddy current problem in the time harmonic case

$$\int_\Omega \mu^{-1} \ \operatorname{curl} \boldsymbol{A} \ \operatorname{curl} \boldsymbol{v} \ d\Omega + \int_\Gamma \mu^{-1} \ \operatorname{curl} \boldsymbol{A} \times \boldsymbol{v}\boldsymbol{n} \ d\Gamma + j\omega \int_{\Omega_m} \sigma \boldsymbol{A}\boldsymbol{v} \ d\Omega = \int_{\Omega_0} \boldsymbol{J}_0 \boldsymbol{v} \ d\Omega.$$

Homogeneous boundary conditions on Γ_H and $\boldsymbol{v} \times \boldsymbol{n} = \boldsymbol{0}$ on Γ_B lead to the finite element approximation:
Find $\boldsymbol{A}_h \in V_B := \{\boldsymbol{A}_h \in \mathcal{V}_h : \boldsymbol{A}_h \times \boldsymbol{n} = \alpha_h \text{ on } \Gamma_B\}$, such that

$$\int_\Omega \mu^{-1} \operatorname{curl} \boldsymbol{A}_h \operatorname{curl} \boldsymbol{v}_h \, d\Omega + j\omega \int_\Omega \sigma \boldsymbol{A}_h \boldsymbol{v}_h \, d\Omega = \int_{\Omega_0} \boldsymbol{J}_0 \boldsymbol{v}_h \, d\Omega \tag{17}$$

for all $\boldsymbol{v}_h \in V_0 := \{\boldsymbol{v}_h \in \mathcal{V}_h : \boldsymbol{v}_h \times \boldsymbol{n} = \boldsymbol{0} \text{ on } \Gamma_B\}$, where $\mathcal{V}_h$ is a finite element subspace of $H(\operatorname{curl}, \Omega)$. The index h indicates a finite element discretization.
For regularization a penalty term is added in air, where $\sigma = 0$, to get an unique solution.

3. TSFEM FOR THE EDDY CURRENT PROBLEM

The TSFEM developed in this work is described here.

3.1 Two-scale approach

The eddy current distribution in laminates in a 2D reference problem was studied in (Hollaus and Schöberl (2010)). Let the x-axis be perpendicular to the lamination as shown in Fig. 1. Eddy currents due to the main magnetic flux are confined to flow in narrow loops. They exhibit essentially a tangential component $\boldsymbol{J}_t$ parallel to the lamination, $\boldsymbol{J}_y$ and $\boldsymbol{J}_z$ according to our assumptions, except at the edges of the laminates, where the eddy currents "turn around" and the normal component $\boldsymbol{J}_n$, i.e. $\boldsymbol{J}_x$, dominates. Based on these observations the two-scale approach

$$\boldsymbol{A} = \boldsymbol{A}_0 + \phi \begin{pmatrix} A_1 \\ A_2 \\ A_3 \end{pmatrix} + \nabla(\phi w) \tag{18}$$

has been developed. In (18) $\boldsymbol{A}_0$ represents the mean value, ϕ times the vector with the entries A_1, A_2 and A_3 models currents parallel to the laminations and the last term in (18) takes account of the normal component of the

current density. The quantities A_1, A_2, A_3 and w are scalar functions. The behavior of the micro-shape function ϕ in x-direction is sketched in Fig. 2, it is constant in the y- and z-direction.

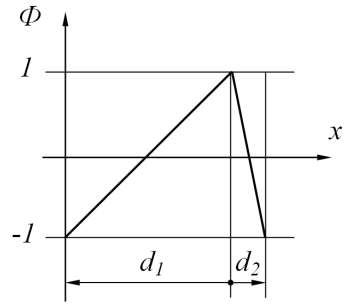

Fig. 2. Periodic micro-shape function $\phi(x)$

Inserting (18) into (16) and integrating by parts leads to the symmetric bilinear form

$$\int_\Omega \mu^{-1}\Big[\operatorname{curl}\big(\boldsymbol{A}_0+\phi(A_1,A_2,A_3)^T+\nabla(\phi w)\big) \cdot \operatorname{curl}\big(\boldsymbol{v}_0+\phi(v_1,v_2,v_3)^T+\nabla(\phi q)\big)\Big]\,d\Omega + j\omega\int_\Omega \sigma\Big[\big(\boldsymbol{A}_0+\phi(A_1,A_2,A_3)^T+\nabla(\phi w)\big) \cdot \big(\boldsymbol{v}_0+\phi(v_1,v_2,v_3)^T+\nabla(\phi q)\big)\Big]\,d\Omega=0, \quad (19)$$

where the test functions v_1, v_2, v_3 and q vanish in Ω_0.
Numerical experiments have shown that neglecting the derivatives of $(A_1, A_2, A_3)^T$ yields a more accurate solution. A rigorous analysis will be presented in a subsequent paper.
Taking the curl of (18) requires the directional derivative $\frac{\partial\phi(s)}{\partial s}\cdot\boldsymbol{n}$ for an arbitrary orientation of the laminates, where $\boldsymbol{n}=(n_x,n_y,n_z,)^T$ means the normal vector to the lamination.
Simple manipulations and neglecting the derivative of A_1, A_2 and A_3, the first integral in (19) reads as

$$A(\overline{\boldsymbol{A}}_0,\overline{A}_1,\overline{A}_2,\overline{A}_3;\overline{\boldsymbol{v}}_0,\overline{v}_1,\overline{v}_2,\overline{v}_3) = \int_\Omega \begin{pmatrix}\operatorname{curl}\overline{\boldsymbol{A}}_0\\ \overline{A}_1\\ \overline{A}_2\\ \overline{A}_3\end{pmatrix}^T \overline{S} \begin{pmatrix}\operatorname{curl}\overline{\boldsymbol{v}}_0\\ \overline{v}_1\\ \overline{v}_2\\ \overline{v}_3\end{pmatrix} d\Omega. \quad (20)$$

The coefficients in $\overline{S}$ were averaged across the laminations as shown in Hollaus and Schöberl (2010). Averaged coefficients and quantities are indicated by the bar. Homogenization takes place by averaging the coefficients over the period with the length $d=d_1+d_2$. The detailed matrix $\overline{S}$ can be found in Appendix A. The second integral in (19) yields

$$B(\overline{\boldsymbol{A}}_0,\overline{A}_1,\overline{A}_2,\overline{A}_3,\overline{w};\overline{\boldsymbol{v}}_0,\overline{v}_1,\overline{v}_2,\overline{v}_3,\overline{q}) = j\omega\int_\Omega \overline{\boldsymbol{A}}^T\ \overline{M}\ \overline{\boldsymbol{v}}\ d\Omega, \quad (21)$$

after similar manipulations as for (19), where

$$\overline{\boldsymbol{A}}=\big((\overline{\boldsymbol{A}}_0)_x,(\overline{\boldsymbol{A}}_0)_y,(\overline{\boldsymbol{A}}_0)_z,\overline{A}_1,\overline{A}_2,\overline{A}_3,\overline{w},\partial_x\overline{w},\partial_y\overline{w},\partial_z\overline{w}\big)^T$$

and

$$\overline{\boldsymbol{v}}=\big((\overline{\boldsymbol{v}}_0)_x,(\overline{\boldsymbol{v}}_0)_y,(\overline{\boldsymbol{v}}_0)_z,\overline{v}_1,\overline{v}_2,\overline{v}_3,\overline{q},\partial_x\overline{q},\partial_y\overline{q},\partial_z\overline{q}\big)^T,$$

respectively. The detailed matrix $\overline{M}$ can be found in Appendix A.
Considering (20) and (21) the finite element formulation for the TSFEM reads as follows:
Find

$(\overline{\boldsymbol{A}}_{0h},\overline{A}_{1h},\overline{A}_{2h},\overline{A}_{3h},\overline{w}_h)\in V_\alpha :=$
$\{(\overline{\boldsymbol{A}}_{0h},\overline{A}_{1h},\overline{A}_{2h},\overline{A}_{3h},\overline{w}_h)\ :\ \overline{\boldsymbol{A}}_{0h}\in\mathcal{U}_h,\ \overline{A}_{1h},\ \overline{A}_{2h},\ \overline{A}_{3h}\in\mathcal{V}_h,\ \overline{w}_h\in\mathcal{W}_h$ and $\overline{\boldsymbol{A}}_{0h}\times\boldsymbol{n}=\boldsymbol{\alpha}_h$ on $\Gamma\}$,
such that

$$A(\overline{\boldsymbol{A}}_{0h},\overline{A}_{1h},\overline{A}_{2h},\overline{A}_{3h};\overline{\boldsymbol{v}}_{0h},\overline{v}_{1h},\overline{v}_{2h},\overline{v}_{3h})+ B(\overline{\boldsymbol{A}}_{0h},\overline{A}_{1h},\overline{A}_{2h},\overline{A}_{3h},\overline{w}_h;\overline{\boldsymbol{v}}_{0h},\overline{v}_{1h},\overline{v}_{2h},\overline{v}_{3h},\overline{q}_h)=0$$

for all
$(\overline{\boldsymbol{v}}_{0h},\overline{v}_{1h},\overline{v}_{2h},\overline{v}_{3h},\overline{q}_h)\in V_0 := \{(\overline{\boldsymbol{v}}_{0h},\overline{v}_{1h},\overline{v}_{2h},\overline{v}_{3h},\overline{q}_h)\ :$
$\overline{\boldsymbol{v}}_{0h}\in\mathcal{U}_h,\overline{v}_{1h},\ \overline{v}_{2h},\ \overline{v}_{3h}\in\mathcal{V}_h,\ \overline{q}_h\in\mathcal{W}_h$ and $\overline{\boldsymbol{v}}_{0h}\times\boldsymbol{n}=\boldsymbol{0}$ on $\Gamma\}$,
where $\mathcal{U}_h$ is a finite element subspace of $H(\operatorname{curl},\Omega)$, $\mathcal{V}_h$ a finite element subspace of $L_2(\Omega_m)$ and $\mathcal{W}_h$ a finite element subspace of $H^1(\Omega_m)$, respectively. The index h stands for finite element discretization, and $\boldsymbol{\alpha}_h$ represents inhomogeneous Dirichlet boundary conditions. The micro-shape function ϕ is in the space of periodic and continuous functions $H_{per}(\Omega_m)$.
Higher order finite elements have been used for the discrete mixed finite element space. The polynomial order of the basis have been chosen according to the de-Rham complex (see Schöberl and Zaglmayr (2005). The L_2 unknowns and all other higher order degrees of freedom are efficiently eliminated on the finite element level building the Schur-complement system. Thus, the number of unknowns of the whole system is reduced significantly.

4. THE LINEAR FEM BENCHMARK

The *Linear FEM Benchmark* consists of a laminated stack with the dimensions of $0.2\times0.1\times0.3$m according to $x\times y\times z$, (see Fig. 3), arranged symmetrically in the center of the race track coil. The thickness of the laminates equals to $0.35mm$, which leads to 556 laminates in the entire stack. A fill factor of $f=0.9722$, a relative permeability of $\mu_r=1,000$, $\mu_r=10,000$ and $\mu_r=30,000$, respectively, an electric conductivity of $\sigma=2\cdot10^6 S/m$ and a frequency of $50Hz$ were selected. Due to three planes of symmetry ($x=0$, $y=0$ and $z=0$), only an eighth of the entire problem was considered in the FEM model. The gap between the laminations was assumed to be air. The height of the race track coil was set to 0.4m, the length and the thickness of the straight sections are 0.2m and 0.05m, respectively. The inner and the outer radius of the four hollow cylinder parts in the corners of the race track coil are 0.01m and 0.06m, respectively. The height of the race track coil was selected essentially larger than the length of the laminated stack to avoid that the eddy currents due to the stray field predominate those caused by the main magnetic flux. A current density of $10^6 A/m^2$ in the coil was chosen.
To study the accuracy of TSFEM and the ansiotropic model the eddy current losses are compared with those obtained by the reference model in which the laminates are modeled individually. The benchmark is small, so that the computational costs of the simulation are still reasonable.

The results are summarized in table 1, where RS stands for reference solution and AS means the solutions of models with anisotropic material properties. To compute RS a preconditioned conjugate gradient method was applied, AS and TSFEM were solved by a direct solver. The computations have been carried out on *numericus* [1] .

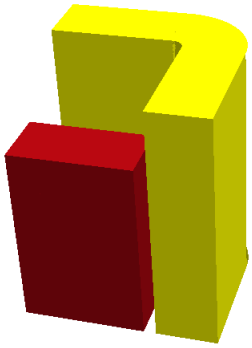

Fig. 3. An eighth of the lamination stack (violet) and the race track coil (yellow).

A comparison of $|\boldsymbol{B}_{max}|$ obtained by AS with that by TSFEM is shown in Fig. 4.

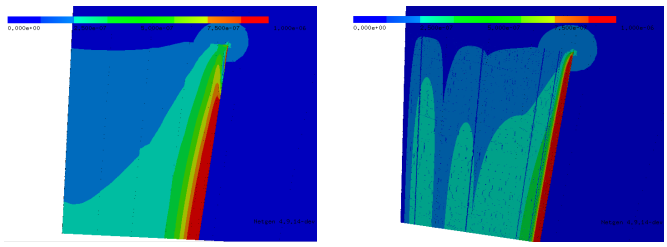

Fig. 4. Solution of $|\boldsymbol{B}_{max}|$, anisotropic solution (left) and two-scal finite element method solution (right).

A fairly good agreement between the TSFEM and the RS can be observed, see table 1. The losses for AS increases with decreasing μ_r, for $\mu_r = 1,000$ the losses of AS are almost equal to that of RS in this benchmark.

Table 1. Eddy Current Losses in W

μ_r	RS	AS	TSFEM
1,000	4.094	4.039	4.248
10,000	1.383	1.201	1.468
30,000	0.952	0.677	1.011

The number of unknowns of the different methods are summarized in table 2. The same finite element model was used for AS and TSFEM. RS requires about 24 times more unknowns than TSFEM. Due to the choice of w in H^1 the number of unknowns in TSFEM is higher than that for AS.

Table 2. No. of Unknowns

RS	AS	TSFEM
14 313 242	411 930	597 597

Finally, the thickness of the laminates d has been scaled down to be $0.001mm$ in TSFEM models. A good agreement can be observed comparing the losses in table 3 with those of AS in table 1. The experiment confirms what one may expect.

Table 3. Experiment: Losses in W

μ_r	TSFEM
1,000	4.047
10,000	1.214
30,000	0.689

[1] *numericus* is a server of 40 cores with 512GByte memory in total.

REFERENCES

Bíró, O., Preis, K., and Ticar, I. (2005). A FEM method for eddy current analysis in laminated media. *COMPEL*, 24(1), 241–248.

De Rochebrune, A., Dedulle, J., and Sabonnadiere, J. (1990). A technique of homogenization applied to the modelling of transformers. *Magnetics, IEEE Transactions on*, 26(2), 520 –523.

Dular, P., Gyselinck, J., Geuzaine, C., Sadowski, N., and Bastos, J.P.A. (2003). A 3-d magnetic vector potential formulation taking eddy currents in lamination stacks into account. *IEEE Trans. Magn.*, 39(3), 1147–1150.

Hollaus and Bíró, O. (1999). Estimation of 3d eddy currents in conducting laminations by an anisotropic conductivity and a 1d analytical solution. *COMPEL*, 18, 494–503.

Hollaus and Bíró, O. (2000). A fem formulation to treat 3d eddy current in laminations. *IEEE Trans. Magn.*, 36(5), 1289–1292.

Hollaus, K. and Schöberl, J. (2010). Homogenization of the eddy current problem in 2d. 14th International IGTE Symposium, Graz, Austria, 154–159. ISBN: 978-3-85125-133-3.

Jack, A. and Mecrow, B. (1987). Calculation of three-dimensional electromagnetic fields involving laminar eddy currents. *Physical Science, Measurement and Instrumentation, Management and Education - Reviews, IEE Proceedings A*, 134(8), 663 –671.

Kaimori, H., Kameari, A., and Fujiwara, K. (2007). Fem computation of magnetic field and iron loss in laminated iron core using homogenization method. *IEEE Trans. Magn.*, 43(4), 1405–1408.

Krähenbühl, L., Dular, P., Zeidan, T., and Buret, F. (2004). Homogenization of lamination stacks in linear magnetodynamics. *IEEE Trans. Magn.*, 40(2), 912–915.

Nogawa, S., Kuwata, M., Nakau, T., Miyagi, D., and Takahashi, N. (2006). Study of modeling method of lamination of reactor core. *IEEE Trans. Magn.*, 42(4), 1455–1458.

Schöberl, J. and Zaglmayr, S. (2005). High order Nédélec elements with local complete sequence properties. *COMPEL*, 24(2), 374–384.

Shin, P.S. and Lee, J. (1997). Magnetic field analysis of amorphous core transformer using homogenization technique. *Magnetics, IEEE Transactions on*, 33(2), 1808 –1811.

Silva, V.C., Meunier, G., and Foggia, A. (1995). A 3d finite element computation of eddy currents and losses in laminated iron cores allowing for the electric and magnetic anisotropy. *IEEE Trans. Magn.*, 31(4), 2139–2141.

Appendix A. MATRICES

The stiffness matrix S is symmetric indicated by the star.

$$\overline{S} = \begin{pmatrix} \overline{\nu} & & & & & & \\ 0 & \overline{\nu} & & & & * & \\ 0 & 0 & \overline{\nu} & & & & \\ 0 & \overline{n_z\phi'\nu} & \overline{-n_y\phi'\nu} & \overline{n_y^2\phi'^2\nu} + \overline{n_z^2\phi'^2\nu} & & & \\ \overline{-n_z\phi'\nu} & 0 & \overline{n_z\phi'\nu} & \overline{-n_xn_y\phi'^2\nu} & \overline{n_x^2\phi'^2\nu} + \overline{n_z^2\phi'^2\nu} & & \\ \overline{n_y\phi'\nu} & \overline{-n_x\phi'\nu} & 0 & \overline{-n_xn_z\phi'^2\nu} & \overline{-n_yn_z\phi'^2\nu} & \overline{n_x^2\phi'^2\nu} + \overline{n_y^2\phi'^2\nu} & \end{pmatrix}$$

The mass matrix M is symmetric indicated by the star.
Averaging of entries multiplied by ϕ cancel out.

$$\overline{M} = \begin{pmatrix} \overline{\sigma} & & & & & & & & & \\ 0 & \overline{\sigma} & & & & & & & & \\ 0 & 0 & \overline{\sigma} & & & & & * & & \\ \overline{\phi\sigma} = 0 & 0 & 0 & \overline{\phi'^2\sigma} & & & & & & \\ 0 & \overline{\phi\sigma} = 0 & 0 & 0 & \overline{\phi'^2\sigma} & & & & & \\ 0 & 0 & \overline{\phi\sigma} = 0 & 0 & 0 & \overline{\phi'^2\sigma} & & & & \\ \overline{n_x\phi'\sigma} & \overline{n_y\phi'\sigma} & \overline{n_z\phi'\sigma} & \overline{n_x\phi\phi'\sigma} = 0 & \overline{n_y\phi\phi'\sigma} = 0 & \overline{n_z\phi\phi'\sigma} = 0 & \overline{\phi'^2\sigma} & & & \\ \overline{\phi\sigma} = 0 & 0 & 0 & \overline{\phi^2\sigma} & 0 & 0 & \overline{n_x\phi'\phi\sigma} = 0 & \overline{\phi^2\sigma} & & \\ 0 & \overline{\phi\sigma} = 0 & 0 & 0 & \overline{\phi^2\sigma} & 0 & \overline{n_y\phi'\phi\sigma} = 0 & 0 & \overline{\phi^2\sigma} & \\ 0 & 0 & \overline{\phi\sigma} = 0 & 0 & 0 & \overline{\phi^2\sigma} & \overline{n_z\phi'\phi\sigma} = 0 & 0 & 0 & \overline{\phi^2\sigma} \end{pmatrix}$$